Available online at www.sciencedirect.com

ScienceDirect

journal homepage: www.elsevier.com/locate/he

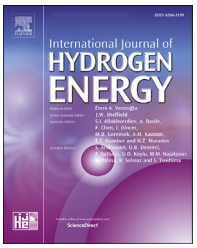

Multi-state optimal power dispatch model for power-to-power systems in off-grid hybrid energy systems: A case study in Spain

A. Martinez Alonso [a,*], G. Matute [b], J.M. Yusta [c], T. Coosemans [a]

[a] Electrotechnical Engineering and Energy Technology, MOBI Research Group, Vrije Universiteit Brussel, Pleinlaan 2, 1050 Brussels, Belgium

[b] DNV, Trovador Buildinjg, Antonio Beltrán Martínez Square, 50002, Zaragoza, Spain

[c] Department of Electrical Engineering, University of Zaragoza, María de Luna, 3, 50018, Zaragoza, Spain

HIGHLIGHTS

- Novel multi-state optimal power dispatch model for power-to-power energy systems.
- Multi-year techno-economic evaluation of an off-grid case study.
- Phasing out fossil fuels with renewable energy-based hybrid energy storage systems.
- Hydrogen technology contributes to a lower levelized cost of energy.
- High initial investment cost was a significant entry barrier to deploying hydrogen.

ARTICLE INFO

Article history:
Received 30 November 2022
Received in revised form
30 May 2023
Accepted 2 June 2023
Available online xxx

Keywords:
Optimal power dispatch
Techno-economic assessment
Power-to-power
Renewable hydrogen
Hybrid energy storage systems
Off-grid

ABSTRACT

The electricity production from Renewable Energy (RE) in isolated locations requires long-term energy storage systems. To that end, Hybrid Energy Storage Systems (HESS), through a combination of hydrogen and batteries, can benefit from the different advantages of both technologies. This paper presents a hybrid Power-to-Power (PtP) Optimal Power Dispatch (OPD) model for isolated systems with no electric grid access. Currently, the electricity supply in such cases is usually based on a mix of RE as the primary energy source sustained by a diesel genset acting as a backup generator. In this context, the model delivers the hourly energy flows between renewable production sources, energy storage devices and the electrical load, which minimises costs and Green House Gases (GHG) emissions. For validation purposes, the model was tested through its application to a case study in an isolated area in the Canary Islands, Spain. The results show that the algorithm calculates the hourly OPD successfully for a given plant sizing, considering the defined operational states of the different assets. These operational constraints showed a decrease in the PtP round-trip efficiency of 5.4% and a reduction of the hydrogen production of 9.7%. Finally, the techno-economic analysis of the results proves that the combination of hydrogen and batteries with RE production is a feasible alternative to phasing out fossil fuels for the selected case study – reducing the diesel generator usage down to 1.2% of the yearly energy supply.

* *Corresponding author.*
E-mail address: ander.martinez.alonso@vub.be (A. Martinez Alonso).

https://doi.org/10.1016/j.ijhydene.2023.06.019

Abbreviations

Acronyms

AM	Ante Meridiem
BB	Battery Bank
BESS	Battery Energy Storage System
DG	Diesel Generator
EPC	Infrastructure and Project Procurement Cost
EU	European Union
FC	Fuel Cell
FCEV	Fuel Cell Electric Vehicle
FCH-JU	Fuel Cells and Hydrogen Joint Undertaking
GHG	Green House Gas
HESS	Hybrid Energy Storage System
H2	Hydrogen
HT	Hydrogen Tank
IPCEI	Important Project of Common European Interest
MES	Multi-Energy Systems
MILP	Mixed-Integer Linear Programming
OPD	Optimal Power Dispatch
PEM	Proton Exchange Membrane
PERC	Passivated Emitter and Rear Cell
PM	Post-Meridiem
PV	Photovoltaic Panel
PtG	Power-to-Gas
PtHtP	Power-to-Hydrogen-to-Power
PtP	Power-to-Power
PtX	Power-to-X (Power-to-Anything)
RE	Renewable Energy
RES	Renewable Energy Sources
SB	Stand-By
TEA	Techno-Economic Assessment
WE	Water Electrolyser
WT	Wind Turbine

Units

(M)W	(10^6) watts [power - energy per unit time]
(k)Wh	(10^3) watts per hour [unit of energy]
(G)W	(10^9) watts [power - energy per unit time]
kg	Kilogram [unit of mass]
m^2	Square metters [unit of area]
m/s	Metters per second [unit of linear speed]
s	Second [unit of time]
h	60 s, hour [unit of time]
EUR	Euros - ε [currency]
y	8760 h, year [unit of time]

Parameters

A	Area [m2]
$P^a_{k,}$	Power [kW]
C^a_k	Charge/discharge C-rate [%]
SOC^a_k	State Of Charge [%]
γ^a_k	Conversion rate [kWh/H_2 kg]
SU^a_k	Start-up [number of cycles]
d	Discount rate [%]
S^a_k	Rated capacity [kWh *or* H_2 kg]
LCOE	Levelised Cost Of Energy [EUR/kWh]
TR	Tax rate [%]
MPL^a	Minimum Partial Load [%]
U	Units [ud.]
NPV	Net Present Value [EUR]
v_v	Speed [m/s]
η^a_k	Efficiency [%]

Variables

a/b^a_i	Operationl state per time step [binary]
$P^a_{i,j}$	Power output per time step [kW]
$CAPEX_i$	Capital Expenditures [EUR/y]
r^a_i	Load factor per time step [%]
CF_i	Cash flows [EUR/y]
R_i	Revenues [EUR/y]
$Curt_i$	Curtailment per time step [kWh]
SI_i	Solar Irradiation per time step [W/m^2]
DA_i	Depreciation and amortization [%]
SOC^a_i	State of Charge per time step [%]
EX^a_i	Expenditures per time step [EUR/y]
$SU\_count^a_i$	Start-up counter [number of cycles]
$Load_i$	Load to supply per time step [kW]
TX_i	Tax payments [EUR/y]
$OPEX_i$	Operational Expenditures [EUR/y]
WS_i	Wind Speed per time step [m/s]

Indices

a	BB, HT, FC, WE, PV, WT [asset]
i	Time step granularity: t, t-1, y [t -hourly, t-1 previous time step, y - yearly]
k	Charge, discharge, nominal, stand-by, idle, maximum, minimum, rated [specific characterization parameter]
v	Minimum (c-in), maximum (c-out) and rated [characterization parameter]

Introduction

As the European Union (EU) 2030 Climate Target Plan aims at cutting greenhouse emissions by 55% below 1990 levels, the policy scenarios foresaw a ramp-up of the installed electrolyser capacity between 37 and 66 GW by 2035 in the EU countries [1]. On top of the "fit for 55" plan for energy transition, the RepowerEU plan increased the budget for hydrogen projects by 300 million euros, setting an additional target of 10 million tonnes of domestic renewable hydrogen production and 10 million tonnes of imports by 2030 to end the EU's dependence on Russian fossil fuels [2]. Furthermore, the first-ever Important Project of Common European Interest (IPCEI) in the hydrogen sector - IPCEI Hy2Tech, was announced in July 2022 with a total investment plan of almost 14.2 billion euros [3]. Consequently, hydrogen has emerged as a sustainable energy

Please cite this article as: Martinez Alonso A et al., Multi-state optimal power dispatch model for power-to-power systems in off-grid hybrid energy systems: A case study in Spain, International Journal of Hydrogen Energy, https://doi.org/10.1016/j.ijhydene.2023.06.019

vector and an alternative to maximizing Renewable Energy (RE) usage in hard-to-abate niche markets [4,5]. Thus, ha variety of projects and research initiatives [6–10] are currently exploring the different potential applications of hydrogen, which are often classified depending on the final end-use.

The term Power-to-X (PtX) refers to the transformation of electricity as the primary energy source into another energy vector, such as heat, cold, or in the case of this article, hydrogen - or even ammonia or methanol [11]. Power-to-Gas (PtG) or Power-to-Hydrogen (PtH) involves hydrogen production with RE via a water-splitting process known as electrolysis [12,13]. Therefore, PtG lies within the scope of PtX and also the further application or conversion of this hydrogen into a third energy vector. Power-to-power (PtP), or power-to-hydrogen-to-power (PtHtP), comprises the generation, storage and further transformation of hydrogen back into electricity through a fuel cell [14]. It can also be found in the literature as one of the applications within the umbrella term PtX [15,16] or in studies that focus on reversible processes such as solid oxide cells [17].

Hydrogen has the potential to become a viable and decarbonised solution for reliable long-term and large-scale storage in different types of energy systems [14,18]. Its low self-discharge rates, stackable capacity, and high energy density [17] enhance its potential and cost-competitiveness as a decarbonised alternative to traditional fossil fuels. It has the potential to reduce the electricity curtailment of off-grid RES-dominated systems [19]. Hydrogen used as energy storage for re-electrification still faces several issues, including high initial investment costs and very low round-trip energy conversion efficiency compared to electrochemical batteries [20,21]. However, often compared, batteries and hydrogen can actually benefit from the combined operational dynamics of both technologies [22,23]. Hybrid Energy Storage Systems (HESS) in power systems subjected to high volatility and uncertainty are rising as a promising application of hydrogen technology thanks to the enhanced synergy when coupled with batteries [24]. Nevertheless, the concept of HESS does not necessarily apply to hydrogen, it has largely researched in the literature, from batteries in combination with fly-wheels [25], batteries and supercapacitors for assisting diesel-fueled maritime applications [26], or simply for the purpose or increasing the battery lifetime [27], to batteries combined with pump storage for maximizing large-scale wind power generation [28]. The competitive advantage of HESS including hydrogen can be found in RE-powered scenarios where large-scale seasonal storage is required [29], for example, when providing flexibility services for the electric grid at the regional or national level [30] or when the unavailability of the electric grid access and balancing services rely on the energy storage systems [31]. Hence, multiple studies have addressed the potential of hydrogen in the configuration of remote off-grid systems. Even though in 2018, its competitiveness versus diesel generators was still arguable [32], more recent studies have proved the cost-effectiveness of hydrogen for long-term storage, increasing the stability of energy systems with high penetration of renewables, reducing the size of Battery Energy Storage Systems (BESS) and reducing the cost and environmental impact versus diesel generators in backup power generation [29,33–35].

Traditionally, in optimal design and operation problems, the modelling of Multi-Energy Systems (MES) [36] has been achieved through power limits that consider the continuous dynamics of the involved assets [37]–[41]. The discrepancy arises regarding the specific power dispatch modelling strategy of HESS. While valid and broadly applied to BESS-dominated MES [41,42], this approach risks being too simplistic for the modelling of hydrogen technology [43]. For example, when combining hydrogen with other vectors multi-objective models are often found in literature, such as biomass waste and water [44], heat, cooling and thermal storage [45], or yet again batteries and hydrogen [46]. However, if a higher level of characterization is desired, the operational aspects need to be addressed, frequent cold start-up cycles could greatly impact the degradation of the equipment [47,48]. Nevertheless, the implications of the intermediate states of operation exceed the scope of degradation and lifetime prediction models. Previous research addressed this debate and found that detailed modelling of the operational states and efficiency of electrolysers can greatly impact the results of the optimal dispatch strategy – with a 13.5% yearly reduction of hydrogen production compared to a simplified model [49], or effect on the minimal partial load depending on the stack consideration [19]. Even when broadening the analysis to MES hubs, the application of partial-load efficiencies and minimum run times had a big impact on the modelling results [50]. Therefore, accurate modelling is a desirable aspect when optimising hydrogen technology's power dispatch, and different authors have integrated these aspects for PtG or PtG systems. Different approaches were found depending on the application of the electrolyser. For example, consideration of intermediate states of operation, such as 'on', 'hot-standby' and 'idle', were addressed for grid flexibility services [51], even though assumptions were applied to reduce the complexity of the formulation by neglecting the idle state. Furthermore, the same authors, in a more detailed model, studied the operation of electrolysers under dynamic conditions, this time considering the previously defined three operational states, while addressing the effect of cold starts was addressed by limiting its number [52]. However, both these optimal power dispatch algorithms were limited by the time resolution, only managing to solve 3–6 days long windows. A similar case was found in a model for the direct integration of electrolysers with wind turbines. However, in this case, the intermediate states were neglected by detailed thermal modelling with ramp-up and ramp-down constraints of the electrolyser [53].

Specifically regarding PtP, most of the power dispatch strategies regarding hydrogen technology were found in the mobility field. The implementation of complex powertrain architectures for fuel-cell electric vehicles (FCEVs) relies on different energy management systems and multi-level control that address the operational complexity of HESS with different dynamics, namely supercapacitors, batteries and the assembly of hydrogen storage with fuel-cell [54]. For instance, a study took into account operational constraints such as up/down ramping of the assets [55]. Then, concerning stationary applications, only a few sequential models for model predictive control have attempted to consider the dynamics and real operational conditions of hydrogen equipment by assuming different states for optimal operation [56]. In this line, more

Please cite this article as: Martinez Alonso A et al., Multi-state optimal power dispatch model for power-to-power systems in off-grid hybrid energy systems: A case study in Spain, International Journal of Hydrogen Energy, https://doi.org/10.1016/j.ijhydene.2023.06.019

efforts should be made towards facilitation hydrogen deployment in off-grid settings [57].

Therefore, we conclude that the level of characterisation of existing literature regarding PtP OPD models for HESS can be further explored. Characterising the operational constraints of hydrogen technology is key to accounting for the lower efficiency and reduced power output during transitions between states, even to considering and/or limiting the number of cold-starts of the equipment, which could affect the lifetime of the equipment. In the end, the real operation of the assets needs to be considered in the modelling of the assets. Then summarising, the novelty of the present paper is found in the following key aspects.

- Novel multi-state optimal power dispatch model for off-grid power-to-power hybrid energy storage systems, including a diesel generator, batteries, electrolyser, hydrogen storage and fuel cell.
- Development of an optimal power dispatch model for year-long window simulations with hourly granularity, enabling further multi-year techno-economic assessment.
- Consideration of operational constraints in the modelling: transition between intermediate states of operation and minimum partial loads, as well as differentiation between warm and cold start-ups – limiting these last ones.
- Validation of the model through application to a real case study, followed by extensive techno-economic analysis.

To this end, the paper is structured as follows: (i) Section 'Introduction' describes the context and state of the art. (ii) Section 'Methodology and Mathematical formulation of the model' describes the algorithm and equations composing the model. (iii) Section 'Case study: The Remote project' shows the application of the model to a case study as a means to probe its performance. (iv) Section 'Results and discussion' presents the techno-economic results achieved by applying the OPD model to the case study. (v) Section 'Conclusions' introduces the lessons learnt and future research steps.

Methodology and mathematical formulation of the model

The methodology developed and proposed in this paper is based on an OPD model for hourly load follow-up over a yearly simulation. Furthermore, financial indicators for applying the model to a broader Techno-Economic Assessment (TEA) are presented. The model considers all elements, including photovoltaic panels (PV), wind turbines (WT), battery banks (BB), diesel genset (DG), water electrolysers (WE), hydrogen tanks (HT) and fuel cells (FC). The assembly of BESS or BB, WE, HT and FC will be referred to as HESS (see Fig. 1)

The mathematical formulation of the model has been divided into different sections referring to the objective function, the data input and the various assets. These were modelled based on different sets of parameters ($Parameter^{asset}$), variables – which were denoted as a function over time ($Variable_{(t)}^{asset}$), constraints and equations that were applied to characterise their operations and physical behaviour. Nevertheless, some general assumptions were made upon the characterisation of the assets: non-linear or quadratic efficiencies were not considered, and effects from self-discharge and degradation of energy storage systems were neglected.

Regarding the definition of the different variables, all the operational states applying to all assets were defined as booleans. Furthermore, the state of charge and load factor were defined as reals between 0 and 1 – which also applied to all the parameters defined as percentual values: asset efficiencies, minimum partial loads (MPL), minimum and maximum capacities, transition times and charge/discharge current rates. At last, regarding the power balance equations, loads were considered positive and generators negative (PV, WT, BB in discharge and FC), following the passive sign convention.

Given the nature of the problem, combining linear functions with quadratic constraints and continuous and discrete variables, the algorithm was formulated based on Mixed-Integer Linear Programming (MILP). The problem was

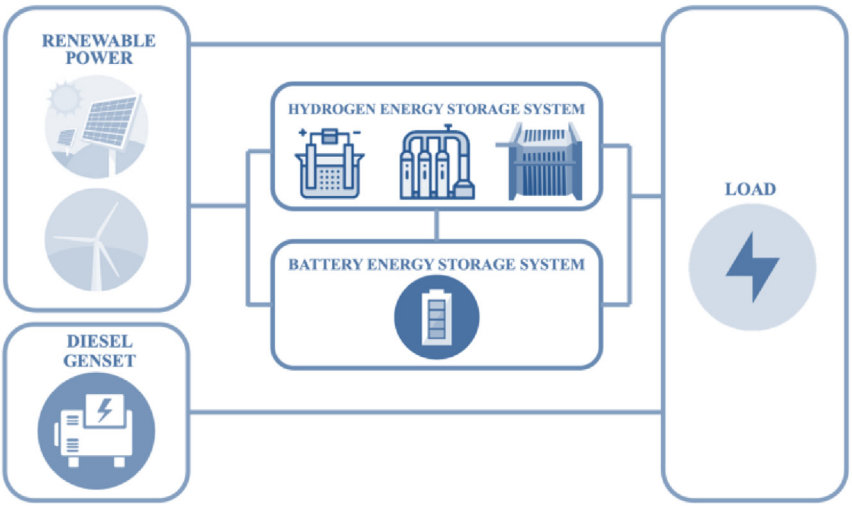

Fig. 1 – Layout of the energy system model.

Please cite this article as: Martinez Alonso A et al., Multi-state optimal power dispatch model for power-to-power systems in off-grid hybrid energy systems: A case study in Spain, International Journal of Hydrogen Energy, https://doi.org/10.1016/j.ijhydene.2023.06.019

written in Python by means of the Pyomo framework and solved using Gurobi.

Objective function

The objective function of the optimisation in Equation (1) contains the expression of the Net Present Value (NPV), calculated as the minimisation of project Expenditures ($EX^{asset}_{(t)}$) sum for a whole year-long hourly simulation – 8760-time steps.

$$NPV = min\left(\sum_{t=0}^{8759} EX^{PV}_{(t)} + EX^{WT}_{(t)} + EX^{WE}_{(t)} + EX^{FC}_{(t)} + EX^{BB}_{(t)} + EX^{DG}_{(t)}\right) \quad (1)$$

Detailed calculation methodology of the NPV applied to a multi-year financial model can be found in Equations (25–27). As per the OPD optimisation problem, since Capital Expenditures (CAPEX) and Operational Expenditures (OPEX) values are constant yearly terms, they are neglected in the optimisation problem. Therefore, the OPD optimised the NPV based on the project hourly cash flows ($CF_{(t)}$), which for a given PtP energy system, means the minimisation of all variable costs affected by the power dispatch.

Power balance

The power balance in Equation (3) addressed the balance of power for every asset ($P^{asset}_{(t)}$) in every time step for the given $Load_{(t)}$. $Curt_{(t)}$ denoted the excess of RE power that could not be stored. Then, as per the units, the model was written in kilowatts (kW),. Furthermore, the time step selected for the model was hourly; hence results were directly expressed in kilowatts per hour (kWh).

$$Load_{(t)} + P^{PV}_{(t)} + P^{WT}_{(t)} + P^{DG}_{(t)} + P^{BB}_{(t)} + P^{WE}_{(t)} + P^{FC}_{(t)} + Curt_{(t)} = 0 \quad (2)$$

Data input – load, PV and WT

The load profile of the target energy system, $Load_{(t)}$, as well as the power output of the RE sources PV and WT: $P^{PV}_{(t)}$ and $P^{WT}_{(t)}$, are known inputs based on historical data, thus known in advance to set the OPD. Wind Speed ($WS_{(t)}$) and Solar Irradiation ($SI_{(t)}$) were used for the calculation of the $P^{PV}_{(t)}$ and $P^{WT}_{(t)}$ curves, as indicated in Equations (3) and (4). Different parameters applied in the calculation, namely, efficiency (η), area per unit (A) and the number of solar panels (u) for the PV, and the minimum (v_{c-in}), maximum (v_{c-out}) and rated (v_{rated}) wind speeds, and the rated power (P_{rated}) for the WT.

$$P^{PV}_{(t)} = \frac{SI_{(t)} \cdot \eta \cdot A \cdot u}{1000} \quad (3)$$

$$P^{WT}_{(t)} = \frac{P_{rated} \cdot (WS_{(t)} - v_{c-in})}{(v_{rated} - v_{c-in})} \quad (4)$$

Battery bank

The power output of the battery was modelled in Equations (5)–(7) based on its two possible operational states – $a^{BB}_{(t)} = 1$ for charging, $a^{BB}_{(t)} = 0$ for discharging, and its physical limits of the maximum power charge and discharge, given as a function of the battery energy storage capacity (S^{BB}_{max}), and its C-rate: C^{BB}_{charge} and $C^{BB}_{discharge}$. Then, Equations (8) and (9) determined the evolution of the State of Charge over time ($SOC^{BB}_{(t)}$), the storage capacity as well as its boundaries ($SOC^{BB}_{min/max}$). For its calculation, charge and discharge efficiencies ($\eta^{BB}_{charge/discharge}$) applied to the charge and discharge power outputs $P^{BB}_{(t),charge}$ and $P^{BB}_{(t),discharge}$, respectively.

$$P^{BB}_{(t)} = a^{BB}_{(t)} \cdot P^{BB}_{(t),charge} + \left(1 - a^{BB}_{(t)}\right) P^{BB}_{(t),discharge} \quad (5)$$

$$0 \le P^{BB}_{(t),charge} \le C^{BB}_{charge} \cdot S^{BB}_{max} \quad (6)$$

$$0 \ge P^{BB}_{(t),discharge} \ge -C^{BB}_{discharge} \cdot S^{BB}_{max} \quad (7)$$

$$SOC^{BB}_{(t)} = SOC^{BB}_{(t-1)} + \frac{a^{BB}_{(t)} \cdot P^{BB}_{(t),charge} \cdot \eta^{BB}_{charge}}{S^{BB}_{max}} + \frac{P^{BB}_{(t),discharge} \cdot \left(1 - a^{BB}_{(t)}\right)}{\eta^{BB}_{discharge} \cdot S^{BB}_{max}} \quad (8)$$

$$SOC^{BB}_{min} \le SOC^{BB}_{(t)} \le SOC^{BB}_{max} \quad (9)$$

Electrolyser and fuel cell

Electrolyser and fuel cell power functions over time ($P^{WE/FC}_{(t)}$) were modelled as in Equations (10–12) - based on their three operational states: on ($a^{WE/FC}_{(t)} = 1$), standby ($b^{WE/FC}_{(t)} = 1$) and idle ($a^{WE/FC}_{(t)} + b^{WE/FC}_{(t)} = 0$). The parameters referring to the nominal power $P^{WE/FC}_{Nominal}$, standby power consumption $P^{WE/FC}_{Standby}$ and idle power consumption $P^{WE/FC}_{Idle}$ applied: The characterisation of these states is further explained and addressed in Fig. 2, below in this section. Additionally, their load factor: $r^{WE/FC}_{(t)}$, and the fraction of a time step spent to transition between idle and on states (TUP^{FC}) was included for the fuel cell

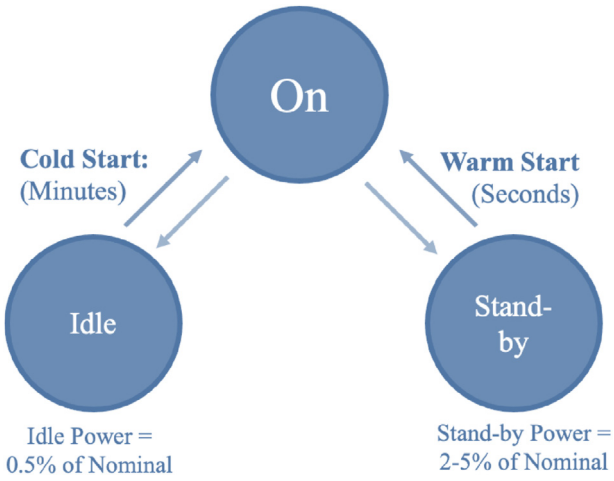

Fig. 2 – Multi-operational state model: On, Standby and Idle.

Please cite this article as: Martinez Alonso A et al., Multi-state optimal power dispatch model for power-to-power systems in off-grid hybrid energy systems: A case study in Spain, International Journal of Hydrogen Energy, https://doi.org/10.1016/j.ijhydene.2023.06.019

function, which experiences a transitory lower power output during the cold start.

$$P_{(t)}^{WE} = P_{Nominal}^{WE}.r_{(t)}^{WE}.a_{(t)}^{WE} + P_{Standby}^{WE}.b_{(t)}^{WE} + P_{Idle}^{WE}.\left(1 - a_{(t)}^{WE} - b_{(t)}^{WE}\right) \quad (10)$$

$$P_{(t)}^{FC} = -P_{Nominal}^{FC}.r_{(t)}^{FC}.a_{(t)}^{FC}.\left(1 - TUP^{FC}.c_{(t-1)}^{FC}\right) + P_{Standby}^{FC}.b_{(t)}^{FC} + P_{Idle}^{FC}.\left(1 - a_{(t)}^{FC} - b_{(t)}^{FC}\right) \quad (11)$$

$$a_{(t)}^{WE/FC} + b_{(t)}^{WE/FC} \leq 1 \quad (12)$$

Then, in equations (13–17), constraints to prevent both simultaneous operation and the transition between idle and standby states, as well as regulating the Minimum Partial Load ($MPL^{WE/FC}$) for the load factor were implemented for both electrolyser and fuel cell:

$$a_{(t)}^{FC} + a_{(t)}^{WE} \leq 1 \quad (13)$$

$$b_{(t)}^{WE/FC} + \left(1 - a_{(t-1)}^{WE/FC} - b_{(t-1)}^{WE/FC}\right) \leq 1 \quad (14)$$

$$\left(1 - a_{(t)}^{WE/FC} - b_{(t)}^{WE/FC}\right) + b_{(t-1)}^{WE/FC} \leq 1 \quad (15)$$

$$r_{(t)}^{WE/FC} - a_{(t)}^{WE/FC} \leq 0 \quad (16)$$

$$-r_{(t)}^{WE/FC} + MPL^{WE/FC}.a_{(t)}^{WE/FC} \leq 0 \quad (17)$$

The definition of the three operational states In Fig. 2 is not arbitrary and follows the described literature in the Introduction.: (i) On: is the state of operation defined by the load factor, minimum partial load and nominal power of the asset. (ii) Standby: In this state, the asset is not operational, although its service conditions are maintained: temperature and pressure. The added value of this state is the possibility of a quick restart of the operation – war start-up. (iii) Idle: in this state, the assets are de-energized, depressurised and at ambient temperature. A residual consumption from the auxiliary systems is considered. In order to switch back to operation, a cold start-up is required.

Additionally, following the declaration of the three operational states, a counter of cold start-ups per optimisation period was included in Equation (18), $SU\_count_{(t)}^{WE/FC}$. The possibility of limiting and/or controlling the number of start-ups was addressed in Equation (19), $SU_{max}^{WE/FC}$.

$$SU\_count_{(t)}^{WE/FC} \geq a_{(t)}^{WE/FC}.\left(1 - a_{(t-1)}^{WE/FC} - b_{(t-1)}^{WE/FC}\right) \quad (18)$$

$$SU_{max}^{WE/FC} \geq \sum_{t=0}^{8759} SU\_count_{(t)}^{WE/FC} \quad (19)$$

Hydrogen tank

The SOC of the hydrogen tank $SOC_{(t)}^{HT}$ was modelled as per Equations (20) and (21). SOC's evolution over time depended on the "On" states of both WE and FC, whose activation filled and depleted the tank. The reduced hydrogen production when transitioning from a cold start-up was also considered TUP^{WE}. Conversion efficiencies - γ^{WE} and γ^{FC} – expressing the ratio of power per kg of hydrogen, and vice versa, for both WE and FC also applied. The storage capacity (S_{max}^{HT}) and its boundaries were also considered ($SOC_{min/max}^{HT}$).

$$SOC_{(t)}^{HT} = SOC_{(t-1)}^{HT} + \frac{P_{Nominal}^{WE}.r_{(t)}^{WE}.a_{(t)}^{WE}}{\gamma^{WE}.S_{max}^{HT}}.\left(1 - TUP^{WE}.\left(1 - a_{(t-1)}^{WE} - b_{(t-1)}^{WE}\right)\right) - \frac{P_{Nominal}^{FC}.r_{(t)}^{FC}.a_{(t)}^{FC}}{\gamma^{FC}.S_{max}^{HT}} \quad (20)$$

$$SOC_{min}^{HT} \leq SOC_{(t)}^{HT} \leq SOC_{max}^{HT} \quad (21)$$

Diesel generator

The diesel genset was modelled in Equation (22) as the power output over time ($P_{(t)}^{DG}$) of a standard generator regulated under a load factor $r_{(t)}^{DG}$ with a nominal power $P_{Nominal}^{DG}$, only limited by a minimum partial load MPL^{DG}. A boolean was used to represent its two possible operational states – $a_{(t)}^{DG} = 1$ for on, and $a_{(t)}^{DG} = 0$ for off. value of the boolean was used to determine the

$$P_{(t)}^{DG} = P_{Nominal}^{DG}.r_{(t)}^{DG}.a_{(t)}^{DG} \quad (22)$$

$$r_{(t)}^{DG} - a_{(t)}^{DG} \leq 0 \quad (23)$$

$$-r_{(t)}^{DG} + MPL^{DG}.a_{(t)}^{DG} \leq 0 \quad (24)$$

Techno-economic assessment: financial indicators

In view of using the OPD model for multi-year TEA purposes, the study of financial indicators was addressed as an additional application of the OPD results. These indicators are the Internal Rate of Return (IRR) and the Levelized Cost Of Energy (LCOE).

The IRR expresses the profitability of the project. It is the value of the discount rate (d) for which the NPV of the project Cash Flows (CF) becomes zero. If it is higher than the desired d value, the project is profitable, and NPV will be higher than zero. Equation (25) presents the calculation of the NPV, considering the lifetime of the facility/project (L), and based on the project's yearly cash flows (CF_y) as per Equation (26). In this equation, R represents the revenues for the electricity produced, and taxes (TX) represent the payment of taxes generated by the operations and investment. Finally, the yearly taxes payments (TX_y) were calculated in Equation (27) as revenues (Ry) minus $OPEX_y$ and minus depreciation and amortization (DA_y), all multiplying the applicable tax rate TR, which is dependent on local conditions.

$$NPV = -CAPEX_0 + \sum_{y=0}^{L} \frac{CF_y}{(1+d)^y} \quad (25)$$

$$CF_y = R_y - OPEX_y - CAPEX_y - TX_y \quad (26)$$

$$TX_y = TR \cdot (R_y - OPEX_y - DA_y) \quad (27)$$

Please cite this article as: Martinez Alonso A et al., Multi-state optimal power dispatch model for power-to-power systems in off-grid hybrid energy systems: A case study in Spain, International Journal of Hydrogen Energy, https://doi.org/10.1016/j.ijhydene.2023.06.019

The LCOE expresses the cost of energy in Equation (28), which was calculated as the total NPV of the project (Equation (25)) divided by the NPV of the energy delivered to Load (E).

$$LCOE = \frac{-CAPEX_0 + \sum_{y=0}^{L} \frac{OPEX_y + TX_y}{(1+d)^y}}{\sum_{y=0}^{L} (E)_y \Big/ (1+d)^y} \quad (28)$$

Case study: The Remote project

The Remote Project is an initiative funded by the European Commission through the Fuel Cells and Hydrogen Joint Undertaking (FCH JU) to demonstrate hydrogen energy storage systems in three remote locations in Spain, Greece and Norway without access to the main electric grid [10]. The Spanish pilot, located on the Canary Island of Gran Canaria, has been selected as a case study for the present paper (see Fig. 3). It comprehends an industrial farm with milking and cooling facilities. The objective of the project is to replace the non-renewable power generation systems, which accounted accounts for 84% of the power generation in the Canary Islands in 2019 [58] - compared to 54% of non-renewable generation for mainland Spain in 2020 [59] – with a decarbonised and sustainable option.

Data input – load, solar irradiation and wind speed profiles

$Load_{(t)}$, $P^{PV}_{(t)}$ and $P^{WT}_{(t)}$ are known inputs for all time periods, shown in Fig. 4. The original daily load profile followed a daily pattern, corresponding to three shifts every 8 h. Therefore it has been extrapolated to a year-long profile with 5% day-to-day and 5% time-step random variability to account for unexpected variations. The meteorological data of 2020 was selected for analysis. The European Union's Earth Observation Programme – Copernicus, which provides high-resolution datasets based on available data from 7 Sentinel satellites and different measurement instruments, was used to extract the data [60].

Objective function and considerations on variable expenses

In the particular case of the REMOTe Project, assumptions were applied to consider the expenditures. Power generation from PV and WT was assumed as free-of-charge, and their fixed CAPEX and OPEX terms were considered the only expenses since the ownership of the assets remained with the kettle farm owner. Furthermore, applying to all assets, CAPEX and OPEX values were neglected from the objective function because those are constant terms; thus, they have no impact on the minimisation of the objective function and the OPD. The cost of maintaining the equipment was assumed to be covered as a yearly cost, represented as a part of the OPEX, compromising preventive and corrective maintenance tasks. Therefore, the replacement cost of the equipment, such as the electrolyser and fuel cell stacks, was assumed independent of its operation. Concluding that the project hourly cash flows were only dependent on the diesel consumed in the genset, as represented by Equation (29). The water cost related to the electrolyser's consumption was neglected in the optimisation due to the relatively smaller cost in comparison to diesel.

$$EX^{DG}_{(t)} = \frac{P^{DG}_{(t)}}{\eta^{DG}} . \eta^{Fuel} . DC^{Fuel} \quad (29)$$

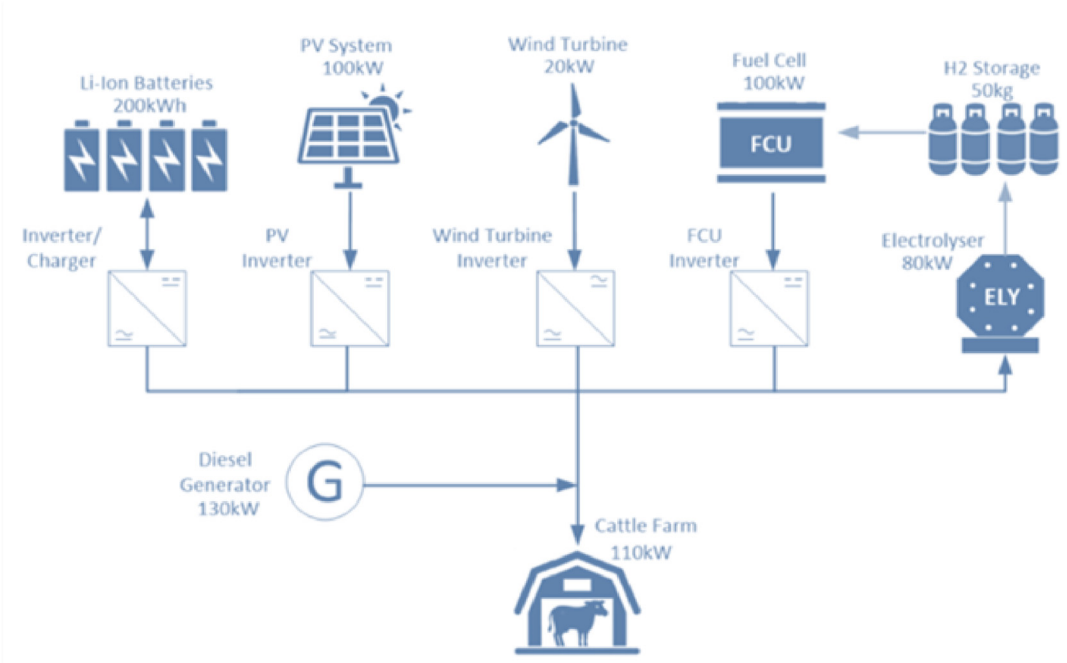

Fig. 3 – Remote's layout – Renewable-powered cattle farm.

Please cite this article as: Martinez Alonso A et al., Multi-state optimal power dispatch model for power-to-power systems in off-grid hybrid energy systems: A case study in Spain, International Journal of Hydrogen Energy, https://doi.org/10.1016/j.ijhydene.2023.06.019

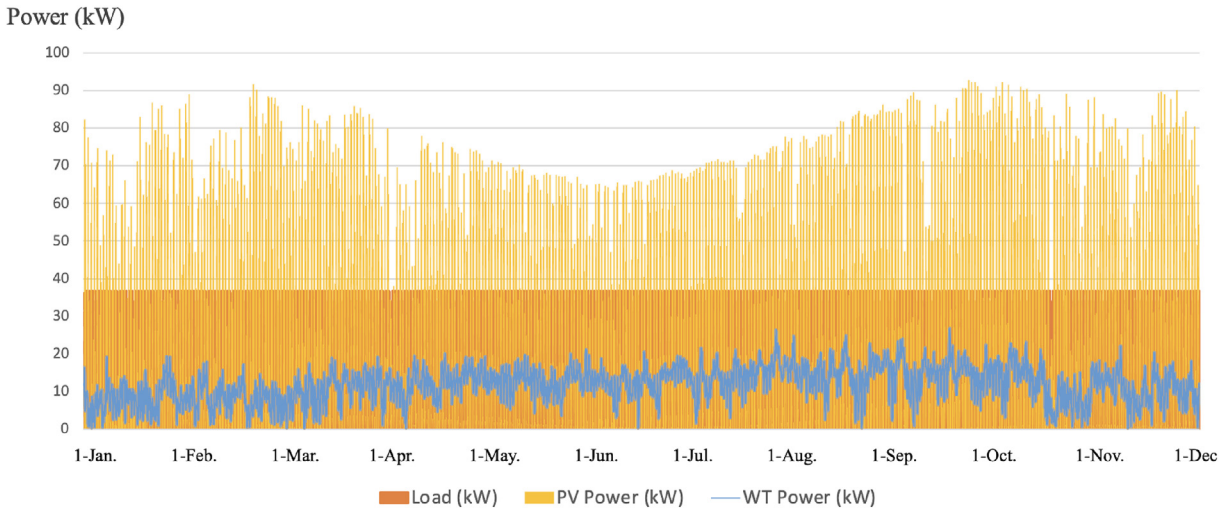

Fig. 4 – Remote's renewable energy generation and load profiles.

Finally, in Equation (30), constant terms were neglected from the function., leaving the expression of the NPV of the project as a function of the power output of the diesel genset, which was to be minimised for the whole year.

$$NPV = min\left(\sum_{t=0}^{8759} P_{(t)}^{DG}\right) \tag{30}$$

Technical and economic data

The techno-economic definition of the assets is part of the model's parameters. For the given case study, the values employed to reproduce the technical and financial results are displayed in Table 1. These values are based on market prices and existing scientific literature. The specifics of the REMOTe project financial information remained confidential.

Per manufacturer guidelines, full equipment replacement costs were considered, being 100% of the initial CAPEX for batteries and diesel genset. However, different assumptions were applied for fuel cells and electrolysers. The replacement cost of the stacks was calculated as a percentage of the original CAPEX: 30%. Then, the rest of the variable costs were annualised as part of the OPEX. This had implications on the operation boundaries of the assets, meaning that a maximum number of cold start-ups per year was enforced. This assumption is based on manufacturer guidelines about the effect of cold start-ups on the equipment's degradation and durability.

Finally, applying to the project, a 20-year lifetime was considered for the calculations, with a 21% tax rate and a 5% inflation rate applicable to all costs. Then, additional costs for engineering and construction work, control station, interconnections and commissioning were given a CAPEX of

Table 1 – Assets technical data overview. Legend: Photovoltaic Panels (PV), Wind Turbines (WT), Battery Banks (BB), Water Electrolyser (WE), Hydrogen Tanks (HT), and Fuel Cells (FC).

Asset [Ref.]	Size	Technical Characteristics	CAPEX (EUR)	OPEX (as % of CAPEX)
PV	100 kW	Passivated Emitter and Rear Cell (PERC) monocrystaline flat plate. 72-cell panels measuring 0.082 m^2. 0.480 kW power output. 20.5% efficiency. Lifetime 25 years.	1000 EUR/kWp	1,5%
WT	20 kW	Tri-blade, direct drive, synchronous generator. Cut-in wind speed: 2.8 m/s, rated wind speed: 7.5 m/s, cut-out wind speed 20 m/s. Lifetime 25 years.	6000 EUR/kW	5%
BB [61,62]	200 kWh	Li-ion battery. C-rate 0.3. Depth Of Discharge (DOD) 80%. Charging efficiency 0.92, discharge efficiency 0.95. Lifetime 4000 cycles	800 EUR/kWh	5%
WE [63,64]	80 kW	Alkaline Electrolyser: 52 kWh/kg H_2 efficiency, 10% minimum load ratio. 30 min cold start-up transition. Nominal power 80 kW, standby consumption 1 kW, idle consumption 0.5 kW. Lifetime 60,000 h.	1400 EUR/kW	3%
HT	30 kg	Type 4 compressed gas: 33,3 kWh per kg of H_2. DOD 80%. Lifetime 25 years.	500EUR/kg	1%
FC [64,65]	100 kW	Proton Exchange Membrane (PEM) fuel cell: 20.94 kWh/kg H_2, 10% minimum load ratio. 15-minute cold start-up transition. Nominal power 120 kW, standby consumption 1.5 kW, idle consumption 0.5 kW. Lifetime: 40,000 h.	1600 EUR/kW	4%
DG [66]	130 kW	ISO 8528 Part 1 Class G3 diesel emergency genset. 60 Hz. Minimum partial load 15%. Lifetime: 30,000 h.	300 EUR/kW	4%

Please cite this article as: Martinez Alonso A et al., Multi-state optimal power dispatch model for power-to-power systems in off-grid hybrid energy systems: A case study in Spain, International Journal of Hydrogen Energy, https://doi.org/10.1016/j.ijhydene.2023.06.019

Table 2 – Sensitivity analysis: Overview of the different design options. Legend: Battery Banks (BB), Electrolyser (EZ), Hydrogen Tanks (HT), and Fuel Cells (FC).

	BB Capacity (kWh)	HT Capacity (kg)	BB C Rate	WE Power (kW)	FC Power (kW)
Base	200	30	0.3	80	100
Case 1	300	30	0.2	80	100
Case 2	300	30	0.3	80	100
Case 3	200	30	0.5	80	100
Case 4	200	50	0.3	80	100
Case 5	200	50	0.3	120	100
Case 6	200	50	0.3	120	60
Case 7	300	50	0.3	120	60
Case 8	300	50	0.2	80	100

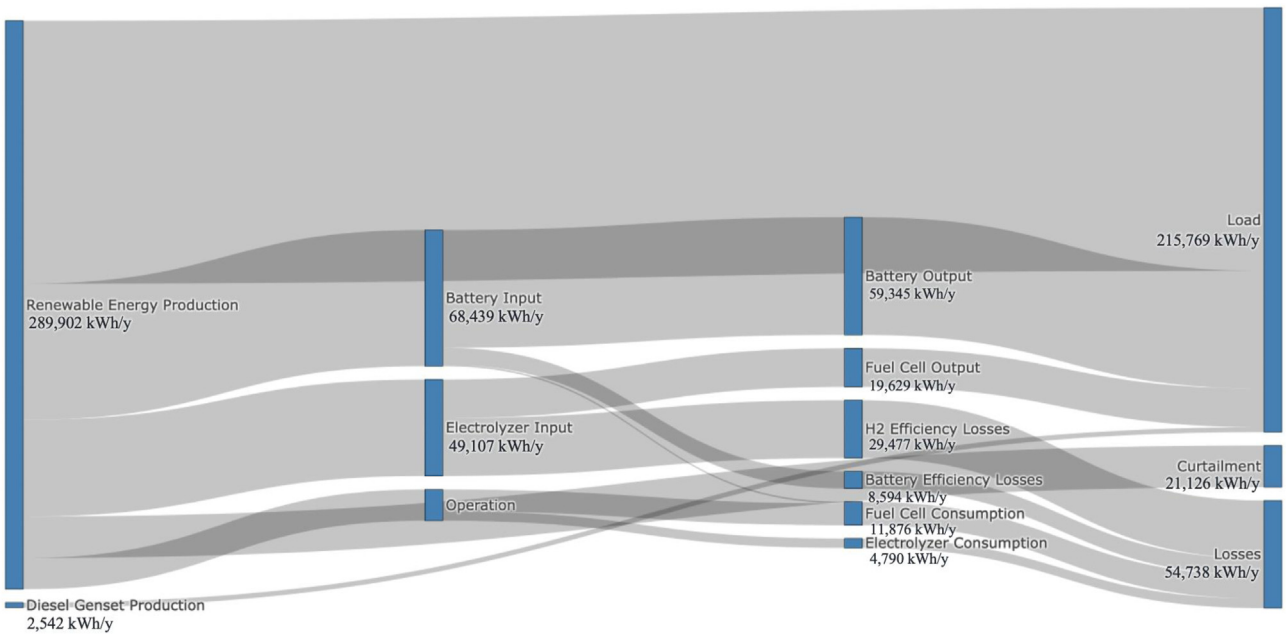

Fig. 5 – Remote's Yearly Energy Dispatch: overview per asset (kWh/y).

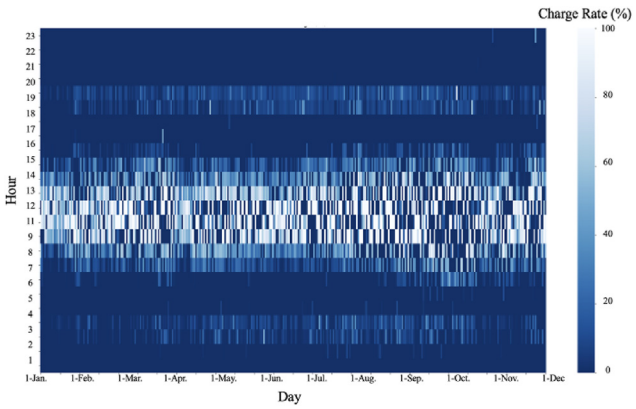

Fig. 6 – Daily variation over a year of the Battery Bank's (BB) load factor (r) while charging.

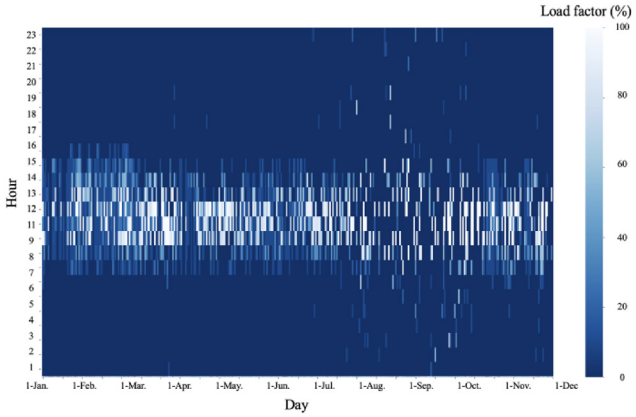

Fig. 7 – Daily variation over a year of the Water Electrolyser's (WE) load factor (r).

Please cite this article as: Martinez Alonso A et al., Multi-state optimal power dispatch model for power-to-power systems in off-grid hybrid energy systems: A case study in Spain, International Journal of Hydrogen Energy, https://doi.org/10.1016/j.ijhydene.2023.06.019

150 k EUR. The cost of water - as the fuel for electrolysis – was considered at 3.8 EUR/m^3, and the cost of diesel – as the fuel for the DG – was 0.39 EUR/kWh.

Sensitivity analysis on multiple HESS designs

Further elaborating on the impact of different design options of the REMOTe project, up to 8 additional cases were developed. These cases comprised various capacities and nominal power values for the assets involved in the HESS (see Table 2).

The objective of the selected sensitivity cases is to, without modifying the layout of the case study, analyse how the optimal dispatch and results vary according to different assets parametrisation involved in the HESS: (1) Increased BB capacity but lower C-rate, (2) Increased BB capacity, (3) Increased BB C-rate, (4) higher HT capacity, (5) Higher HT capacity with bigger WE, (6) Higher HT capacity, bigger ELY and smaller FC, (7) Combination of cases 6 and 2, (8) Combination of cases 1 and 4.

Conversely, the objective of the OPD is to reduce the cost. For the given case study, a stand-alone diesel case was selected as the reference case for all financial indicators and economic calculations. Therefore, the discount rate d for all the scenarios has been set as equal to the IRR value of the diesel stand-alone case. This is, for all scenarios, IRR should be higher than a discount rate equal to the IRR value of the diesel stand-alone case as a minimum to invest in a low emissions alternative. Thus, the discount rate was set at 8%, equal to the IRR of the diesel stand-alone alternative.

Results and discussion

This section first presents the results and analysis of the OPD application to the case study. It follows a discussion of critical aspects of the characterisation, operation and impact of power-to-power hydrogen systems.

Then, in the second step, the financial indicators for the different cases were exhibited and analysed to assess the potential of hydrogen to replace diesel gensets in off-grid energy systems; a hypothetical scenario is also discussed.

Optimal power dispatch strategy

The yearly energy throughputs per asset project are compared in Fig. 5. The load represented a total consumption of 215,769 kW h/y. RE production was calculated at 289,902 kW h/y; therefore, storage systems were vital to enable the flexibility required to supply the load at all times. The battery delivered 59,345 kW h/y of the total load – 27.5% prioritised over the HESS due to an overall roundtrip efficiency of 87.5%. Then, as per the hydrogen, the MILP model showed a 36.6% roundtrip efficiency for the HESS, achieving a yearly output in the FC of 19,629 kW h/y, with a WE energy input of 53,897 kW h/y, of which 4790 kW h/y corresponded to the cost of operation at standby and idle states. In the case of the FC, this consumption accounted for an additional 11,876 kW h/y, which, if taken into account, reduces the total roundtrip efficiency down to 31.4%.

Therefore, we confirm that the detailed operational modelling led to a 5.2% efficiency reduction for the WE-HT-FC pathway in comparison to a simplified model. Regarding the PtG part, the electrolyser additional consumption observed in operation accounted for 4790 kW h/y, which means roughly 9.7% lower hydrogen production than in a simplified model with no operational constraints.

The DG yearly output decreased to 2542 kWh/y, representing only 1.2% of the total load consumption. On the other hand, energy losses represented 25,71% of the entire load – 54,738 kW h/y, and the energy curtailment represented 7.29% of the total RE production - 21,126 kWh/y.

Then, the operation of the different assets was also analysed through their load factor. Figs. 6 and 7 compare the load factor of the WE and BB inputs. Following the higher RE production during the central hours of the day, it is possible to observe how the higher load factors for both assets were allocated at this time range. However, due to the lower roundtrip efficiency of the H_2 storage system and the MPL load of the WE, the battery always starts charging first. This effect was highlighted for those time steps when the load was reduced - between 6 and 8 PM and 2–3 AM.

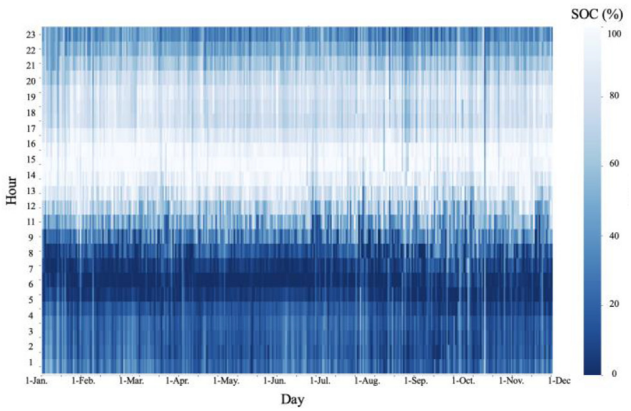

Fig. 8 – Daily variation over a year of the Battery Bank's (BB) State of Charge (SOC).

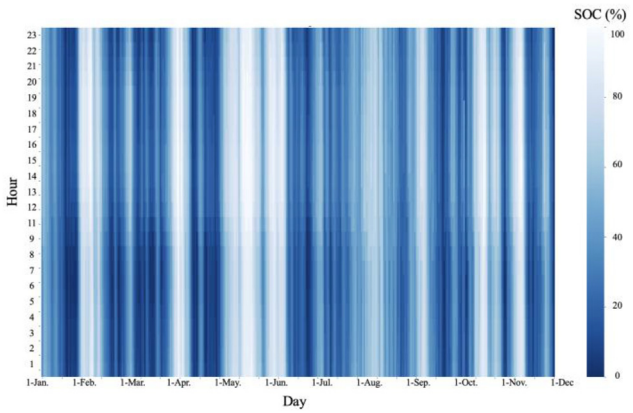

Fig. 9 – Daily variation over a year of the Hydrogen Tank's (HT) State of Charge (SOC).

Please cite this article as: Martinez Alonso A et al., Multi-state optimal power dispatch model for power-to-power systems in off-grid hybrid energy systems: A case study in Spain, International Journal of Hydrogen Energy, https://doi.org/10.1016/j.ijhydene.2023.06.019

Similarly, both BB and HT analysed the State Of Charge (SOC) in Figs. 8 and 9. Results showed the difference in the time range of both storage options. In the case of the BB, the variation of the SOC occurred in the hourly range - vertical axis. Meanwhile, the HT showed a different SOC variation over the year, with unperceivable variations in the hourly range but well-defined transitions on the daily range – horizontal axis.

Furthermore, regarding the FC and BB output when discharging in Figs. 10 and 11, we observe the FC taking an auxiliary role, supplying power mostly at its lower power range: 10–50% when the BB could not cope with the energy demand. This effect was again due to the lower efficiency and limitations regarding the MPL.

Regarding the multi-state operation of WE and FC, the constraint on the maximum number of cold start-ups was respected – 400 a year. Additionally, as shown in Fig. 12, the introduction of the intermediate states proved relevant in the assets' operation. In Fig. 12, the 16th and March 17, 2021 were selected to showcase the performance of these states. The system successfully used the SB state to prioritise the readiness of the asset for a warm start-up over the reduction of its power consumption. In the case of the FC, the SB state was also employed to reduce the number of cold start-ups - hours 8 to 17, or simply following the load overnight, as in hours 17 to 32. Then, regarding the WE, the SB state became relevant when the BB needed to be prioritised for charging, and a cold start wanted to be avoided during peak RE production hour – f. e. hour 12.

Finally, as per the DG in Fig. 13, its role was relegated to peak load procurement when the combination of energy storage and RE production could not follow the load. In this case, given the higher nominal power output of the DG – 130 kW, the effect of the MPL was even more pronounced than in the cases of WE and FC, restricting its operation to only above 19.5 kW. In addition, results showed that the power output of the DG never exceeded 32.5 kW – load factor of 25%, confirming the oversizing of the asset.

Finally, the sensitivity analysis results comprising different design options for the assets involved in the HESS are displayed in Fig. 14.

All the cases where either the C-rate or the battery capacity were increased (1, 2, 7 and 8) experienced a higher reduction of the use of the DG – down to 1110 kWh/y on average, 56.3% less than the base case and only 0.5% of the total yearly load. Battery-dominated HESS proved to achieve better results in terms of dispatch due to the reduced seasonality of renewable resources and daily variability of the load. Additionally, the impact of having higher combined efficiency in the HESS was translated into reduced dependency on larger-scale long-term energy storage. Hence the total share of energy stored was reduced, increasing the percentage of energy curtailed and cutting the FC to half its initial value.

On the other hand, cases where only the design of the hydrogen assets was modified (3, 4, 5 and 6), showed mixed results. However, increasing the hydrogen storage capacity proved an improvement regarding the dispatch of DG, achieving a reduction of 27%. Furthermore, modifications in the FC and WE power capacity did not produce an increased share of H2 in the system's flexibility. The size of the storage and the MPL of the equipment constrained the dispatch of more hydrogen. This last element could be observed through case 6 when a reduction of 40% capacity in the FC produced a 6.5% increase in the FC yearly output.

Financial indicators

The results of IRR and LCOE per scenario are shown in Table 3. Regardless of the HESS design, all the cases proved a more profitable option than investing in a stand-alone diesel facility, given the lower IRR value and higher LCOE obtained.

However, further analysis of the different kinds of costs that participated in the LCOE was performed. As a result, in Fig. 15, the LCOE of each case/scenario was disaggregated into the contributions from CAPEX, OPEX and Taxes (TX). In addition, for a better assessment of the CAPEX, it was further broken down into investments relative to the purchase of the assets, 'Equipment CAPEX', and those associated with other expenses comprising the engineering, procurement and construction of the plant, 'Other EPC expenses'.

All the HESS scenarios proved to be CAPEX-intensive, requiring an initial investment four times higher than the

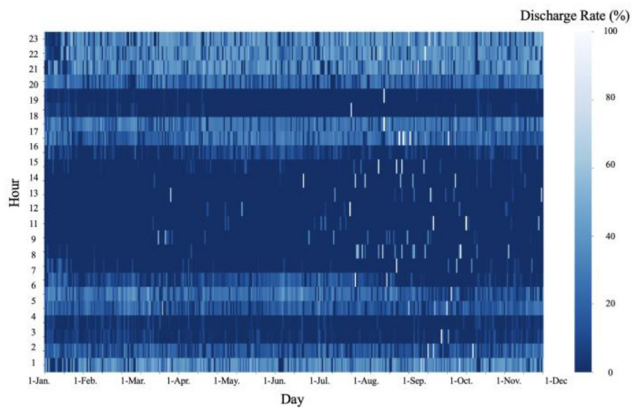

Fig. 10 – Daily variation over a year of the Battery Bank's (BB) load factor (r) while discharging.

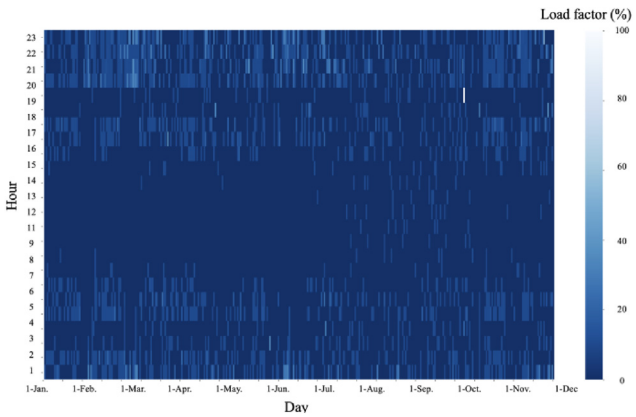

Fig. 11 – Daily variation over a year of the Fuel Cell's (FC) load factor (r).

Please cite this article as: Martinez Alonso A et al., Multi-state optimal power dispatch model for power-to-power systems in off-grid hybrid energy systems: A case study in Spain, International Journal of Hydrogen Energy, https://doi.org/10.1016/j.ijhydene.2023.06.019

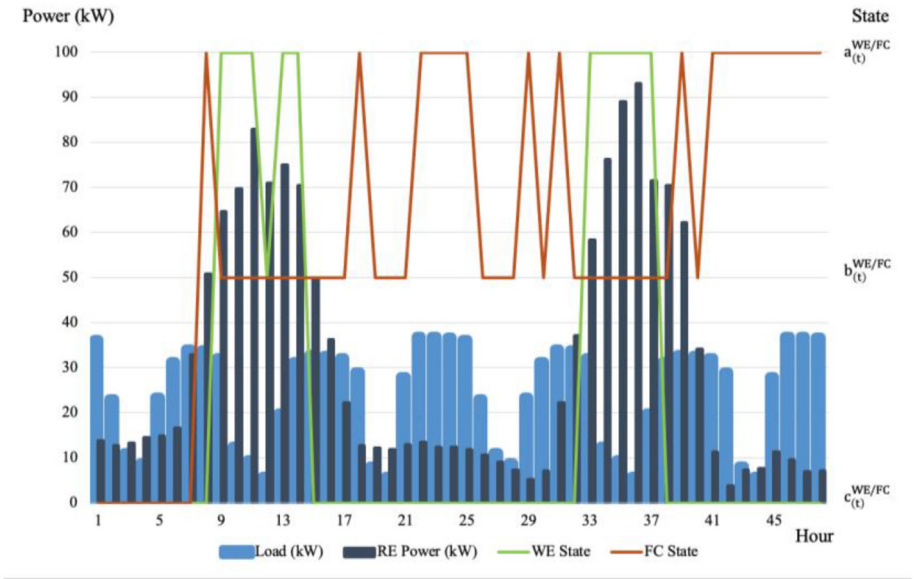

Fig. 12 – 48-h-long window showcasing the multi-state operation of Fuel Cell (FC) and Electrolyser (WE), compared to the Load and the Renewable Energy (RE) power input.

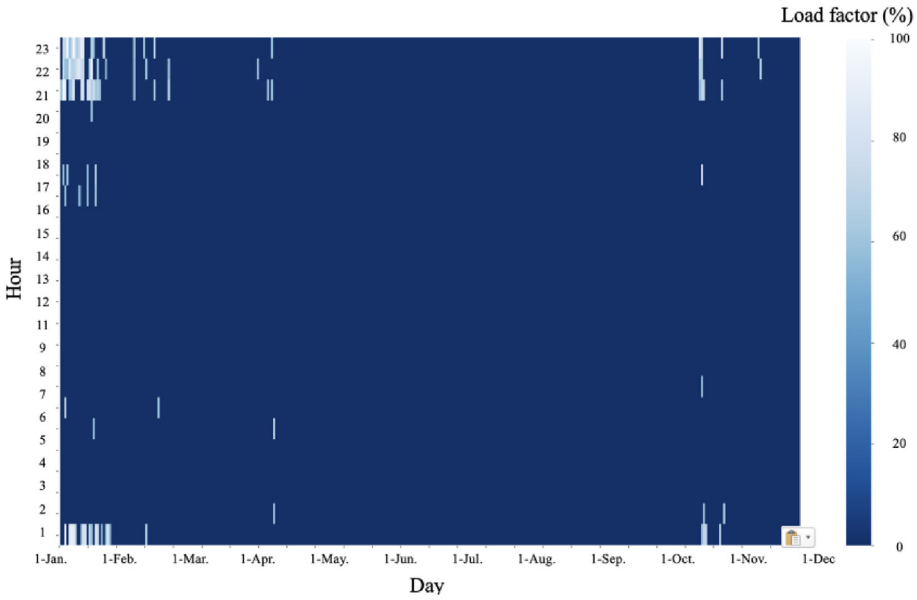

Fig. 13 – Load factor (r) daily variation over a year of the Diesel Genset (DG).

stand-alone diesel design – 0.089 EUR/MWh. In addition to the higher CAPEX-related costs of the low-carbon scenarios, other EPC expenses comprising deployment of engineering, control, integration and commissioning activities, which were not present in the diesel-only scenario, added up on the LCOE value. However, when comparing the weight of the OPEX with the total value of the LCOE, the reliance on an external fuel import proved to be the most critical factor. The stand-alone diesel case, highly affected by the cost of the fuel supply, became the worst case overall – 0.586 EUR/MWh versus 0.150 EUR/MWh on average. Then, as per the impact of taxes, the OPEX-intensive diesel-only case benefitted from the current taxes – 0.012 EUR/MWh compared to 0.068 EUR/MWh on average, partially due to the lack of consideration of carbon taxes.

In Fig. 16, the different low-carbon scenarios were more thoroughly analysed. The LCOE values were analysed and compared to the HESS sizing for every sensitivity case.

The analysis of the different cases showed a variety of results. On one side, cases 1 and 2 did not show any improvement in comparison to the base case. Upscaling the BESS storage capacity allowed for increasing the integration of RE and reducing the dependence on diesel. Still, it also implied higher CAPEX and OPEX values that negatively affected the profitability of the project. In case 3, the C-rate of the battery was increased from 0.3 to 0.5, but the size of the battery remained

Please cite this article as: Martinez Alonso A et al., Multi-state optimal power dispatch model for power-to-power systems in off-grid hybrid energy systems: A case study in Spain, International Journal of Hydrogen Energy, https://doi.org/10.1016/j.ijhydene.2023.06.019

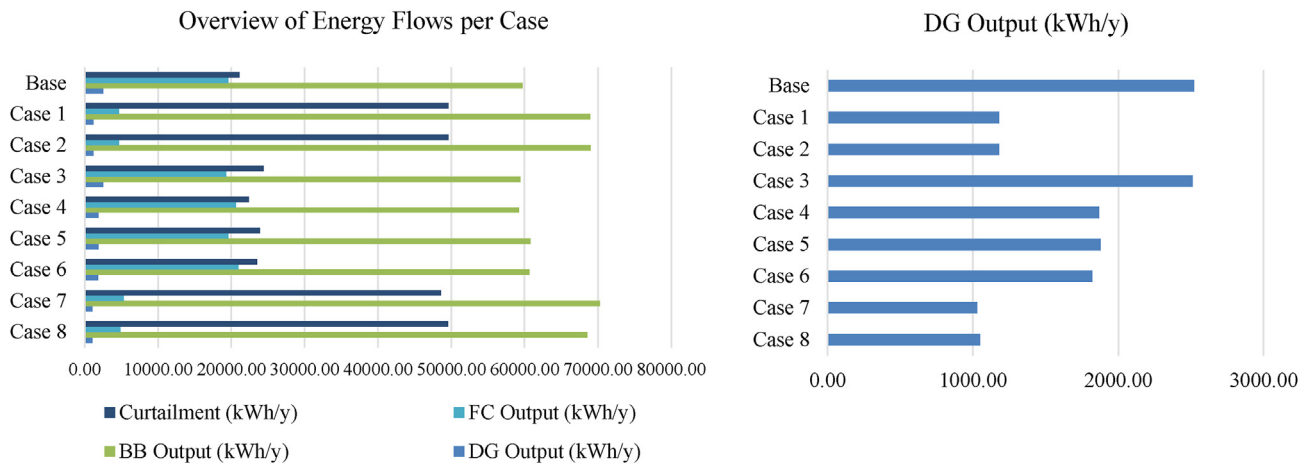

Fig. 14 – Energy flows comparatively per case: Curtailment, Battery Bank (BB), Fuel Cell (FC), and Diesel Genset (DG).

Table 3 – IRR and LCOE values obtained for the scenarios and diesel stand-alone case.

Scenario	Base	1	2	3	4	5	6	7	8	Stand-alone diesel
IRR (%)	9.7	8.5	8.5	9.9	9.8	8.9	9.9	8.5	8.4	8.0
LCOE (EUR/MWh)	0.629	0.669	0.669	0.624	0.628	0.656	0.623	0.669	0.674	0.688

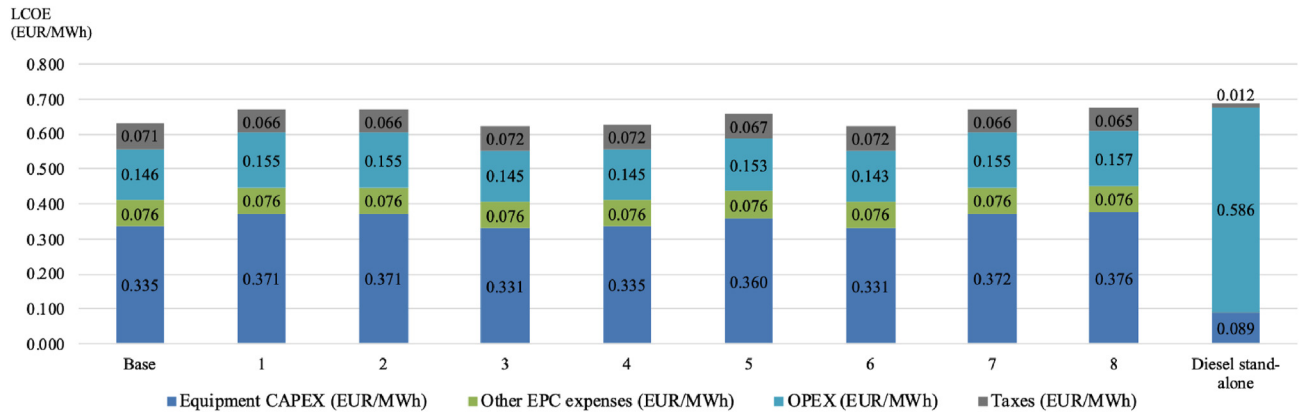

Fig. 15 – Levelized Cost of Energy (LCOE) breakdown into CAPEX (Capital Expenditure) categories, OPEX (Operational Expenditure) and taxes.

equal to the base case. The results showed a small effect on the LCOE value – from 0.629 down to 0.624 EUR/MWh. No effect was perceived in case 1, where the C-rate was reduced to 0.2. Therefore, an increased C-rate proved to be beneficial for the design of the BESS and, thus, the profitability of the project.

On the other side, cases 4, 5 and 6 focused on different sizes of hydrogen assets. Increasing hydrogen storage capacity in all of these, for the same given electrolysis and fuel cell power capacity, was not as cost-intensive in CAPEX as expanding a BESS (scenarios 1 and 2 remained less attractive than the base case). Even though scenario 3 was still a preferable option, increasing the capacity of the HT, as in scenario 4, proved to be a highly profitable and easily achievable solution. Then, scenario 5 varied the size of the electrolyser while keeping the same elements in the rest of the plant. A larger electrolyser increased the integration of RE to cope with seasonality. However, the elevated CAPEX of electrolysis impacted negatively on the total LCOE. A contrary effect was achieved by means of reducing the FC sizing. Scenario 6 led to the best LCOE value thanks to a better design fitting by integrating a smaller FC.

Finally, scenarios 7 and 8 combined previous designs, showing no benefit on the LCOE or IRR. Scenario 6 remained the most cost-competitive - IRR of 9.9%. As it can be observed, the increase of the BESS is not beneficial for the facility above a certain threshold; the same happened with increasing the capacity of the electrolyser. In line with this, scenario 8 was the

Please cite this article as: Martinez Alonso A et al., Multi-state optimal power dispatch model for power-to-power systems in off-grid hybrid energy systems: A case study in Spain, International Journal of Hydrogen Energy, https://doi.org/10.1016/j.ijhydene.2023.06.019

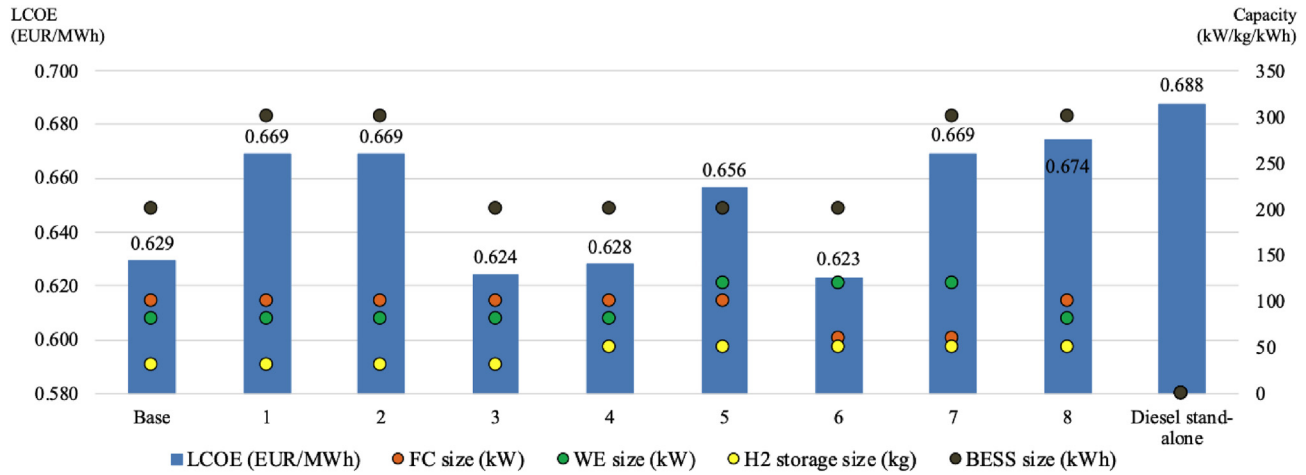

Fig. 16 – Levelized Cost of Energy (LCOE) values about the sizing of the assets: Fuel Cell (FC, kW), Hydrogen Tank (HT, kg), Water Electrolyser (WE, kW) and Battery Energy Storage System (BESS, kWh) for each scenario.

least profitable due to the combined higher CAPEX of the battery and electrolyser, without a real positive impact on the OPD strategy.

Conclusions

The present paper argued the potential of a novel model for OPD of hybrid power-to-power energy systems, including hydrogen, for off-grid conditions. The model combined multiple states of operation for different assets: on, standby and idle for both electrolyser and fuel cell, enabling a higher degree of characterisation of the assets while keeping a more accurate and realistic optimisation of the power dispatch. The novelty was found in the introduction of concepts of operation into design and power dispatch strategies for more realistic outputs. These operational constraints showed a decrease in the PtP round-trip efficiency of 5.4% and a reduction of the hydrogen production of 9.7%. The Remote project case study served as an example of the application of the presented methodology.

Based on the results achieved for the case study presented, the combination of batteries and hydrogen proved to be a viable alternative to fossil fuels in remote locations. Batteries were suited to cover transients and daily storage needs, while hydrogen was the most profitable alternative for long-term and large-scale storage. As shown by the dispatch strategy, the use of diesel in renewable-powered scenarios was relegated to a secondary role for covering load peaks. This auxiliary role proved the cost-competitiveness of RE in combination with HESS versus traditional diesel gensets solely for all sensitivity cases analysed. The optimal scenario showed a 7.7% LCOE reduction - 0.053 EUR/kWh - versus the DG-only reference, with only a 1.5 years increase of the ROI. Also, a low-hanging fruit was identified for the particular case of the Remote project, its performance could be enhanced at a relatively low cost by increasing the size of the HT up to 50 kg.

Furthermore, the sensitivity analysis results proved that both DG and FC assets were oversized and unsuitable for their function in the power dispatch strategy, leading to higher LCOE values. However, the equipment selection is usually subjected to certain particularities and/or by the existence and availability of on-the-shelf equipment suiting the desired power. This was the case with the REMOTte project; however, this issue is expected to remain a singular case as the market segmentation for hydrogen technology grows.

Finally, the role of hydrogen in long-term and large-scale storage was studied. Despite showing better financial indicators than the diesel-based solution cutting down the OPEX down to 25%, the up to 4 times higher CAPEX values were potential entry barriers to deploying the technology. This is because low-carbon plants are typically more complex to execute as they need to integrate different generation and storage assets. This means more expenses on top of the already higher CAPEX of assets. Thus, even with more profitable cases, the CAPEX investments required in these projects are a barrier because those are too high for the limited gain in internal return rate and reduction in LCOE achieved. This is why support for these projects in the form of grants and/or low-interest loans in public funding programmes is important to save the high CAPEX barrier, enabling projects to prove their profitability during their operational phases. Again, this was the case for the REMOTe project.

Declaration of competing interest

The authors declare that they have no known competing financial interests or personal relationships that could have appeared to influence the work reported in this paper.

Acknowledgements

This work is supported by MAMUET an ICON project funded by VLAIO (Flanders innovation & entrepreneurship) under the grant number HBC.2018.0529. This work was developed during a doctoral internship in collaboration with Inycom (Intrumentación y Componentes S.A.), and the REMOTe project funded by the Fuel Cells and Hydrogen 2 Joint Undertaking (now Clean Hydrogen Partnership) under grant agreement

No779541. This Joint Undertaking receives support from the European Union's Horizon 2020 research and innovation programme, Hydrogen Europe and Hydrogen Europe Research.

REFERENCES

[1] European Commission. Impact Assessment, accompanying Communication 'Stepping up Europe's 2030 climate ambition - investing in a climate-neutral future for the benefit of our people.," SWD - staff and joint working documents. European Commission 2020:176. final.
[2] European Commission. RepowerEU: A plan to rapidly reduce dependence on Russian fossil fuels and fast forward the green transition. May, 2022.
[3] E. Commission and C. A. Delivery. Remarks by executive vice-president vestager on important project of Common European interest in the hydrogen technology value chain. July, 2022.
[4] Fuel cells and hydrogen Joint undertaking (FCH). Hydrogen Roadmap Europe; 2019. https://doi.org/10.2843/249013.
[5] IEA. Hydrogen – analysis - IEA. https://www.iea.org/reports/hydrogen. [Accessed 15 December 2021].
[6] Clean Hydrogen Partnership. HyUsPRe. 2021. https://www.clean-hydrogen.europa.eu/projects-repository/hyuspre_en. [Accessed 19 November 2022].
[7] Clean Hydrogen Partnership. MultiPLHY. 2020. https://www.clean-hydrogen.europa.eu/projects-repository/multiplhy_en. [Accessed 19 November 2022].
[8] Clean hydrogen partnership. Haeolus; 2018. https://www.clean-hydrogen.europa.eu/projects-repository/haeolus_en. [Accessed 19 November 2022].
[9] Clean Hydrogen Partnership. HEAVENN. 2020. https://www.clean-hydrogen.europa.eu/projects-repository/heavenn_en. [Accessed 19 November 2022].
[10] Remote project – REMOTE project. https://www.remote-euproject.eu/remote-project/. [Accessed 8 December 2021].
[11] Palys MJ, Daoutidis P. Power-to-X: a review and perspective. Comput Chem Eng Sep. 2022;165. https://doi.org/10.1016/j.compchemeng.2022.107948.
[12] Wang S, Wang S, Zhao Q, Dong S, Li H. Optimal dispatch of integrated energy station considering carbon capture and hydrogen demand. Energy Apr. 2023;269. https://doi.org/10.1016/j.energy.2023.126981.
[13] Fambri G, Diaz-Londono C, Mazza A, Badami M, Sihvonen T, Weiss R. Techno-economic analysis of Power-to-Gas plants in a gas and electricity distribution network system with high renewable energy penetration. Appl Energy Apr. 2022;312. https://doi.org/10.1016/j.apenergy.2022.118743.
[14] El-Shimy M, Profile S, Afandi AN, El-Shimy M. Overview of power-to-hydrogen-to-power (P2H2P) systems based on variable renewable sources total solar radiation on tilted surface view project economics of variable renewable sources for electric power production-a new textbook view project the 5 th international conference on electrical, electronics, and information engineering overview of power-to-hydrogen-to-power (P2H2P) systems based on variable renewable sources. 2017 [Online]. Available: https://www.researchgate.net/publication/319653679.
[15] Sterner M, Specht M. Power-to-gas and power-to-x—the history and results of developing a new storage concept. Energies (Basel) Oct. 2021;14:20. https://doi.org/10.3390/en14206594.
[16] Incer-Valverde J, Patiño-Arévalo LJ, Tsatsaronis G, Morosuk T. Hydrogen-driven Power-to-X: state of the art and multicriteria evaluation of a study case. Energy Convers Manag Aug. 15, 2022;266. https://doi.org/10.1016/j.enconman.2022.115814. Elsevier Ltd.
[17] Buffo G, Ferrero D, Santarelli M, Lanzini A. Reversible Solid Oxide Cell (ReSOC) as flexible polygeneration plant integrated with CO2 capture and reuse. In: E3S web of conferences. EDP Sciences; Aug. 2019. https://doi.org/10.1051/e3sconf/201911302009.
[18] Escamilla A, Sánchez D, García-Rodríguez L. Assessment of power-to-power renewable energy storage based on the smart integration of hydrogen and micro gas turbine technologies. Int J Hydrogen Energy May 2022;47(40):17505–25. https://doi.org/10.1016/j.ijhydene.2022.03.238.
[19] Ibáñez-Rioja A, et al. Off-grid solar PV–wind power–battery–water electrolyzer plant: simultaneous optimization of component capacities and system control. Appl Energy Sep. 2023;345:121277. https://doi.org/10.1016/j.apenergy.2023.121277.
[20] Zhang Y, Campana PE, Lundblad A, Yan J. Comparative study of hydrogen storage and battery storage in grid connected photovoltaic system: storage sizing and rule-based operation. Appl Energy 2017;201:397–411. https://doi.org/10.1016/j.apenergy.2017.03.123.
[21] Belmonte N, et al. A comparison of energy storage from renewable sources through batteries and fuel cells: a case study in Turin, Italy. Int J Hydrogen Energy 2016;41(46):21427–38. https://doi.org/10.1016/j.ijhydene.2016.07.260.
[22] Hemmati R, Mehrjerdi H, Bornapour M. Hybrid hydrogen-battery storage to smooth solar energy volatility and energy arbitrage considering uncertain electrical-thermal loads. Renew Energy 2020;154:1180–7. https://doi.org/10.1016/j.renene.2020.03.092.
[23] Cau G, Cocco D, Petrollese M, Knudsen Kær S, Milan C. Energy management strategy based on short-term generation scheduling for a renewable microgrid using a hydrogen storage system. Energy Convers Manag 2014;87:820–31. https://doi.org/10.1016/j.enconman.2014.07.078.
[24] Marocco P, Ferrero D, Lanzini A, Santarelli M. Optimal design of stand-alone solutions based on RES + hydrogen storage feeding off-grid communities. Energy Convers Manag Jun. 2021;238. https://doi.org/10.1016/j.enconman.2021.114147.
[25] Ngila Mulumba A, Farzaneh H. Techno-economic analysis and dynamic power simulation of a hybrid solar-wind-battery-flywheel system for off-grid power supply in remote areas in Kenya. Energy Convers Manag X Apr. 2023;18. https://doi.org/10.1016/j.ecmx.2023.100381.
[26] Zhang Y, Xue Q, Gao D, Shi W, Yu W. Two-level model predictive control energy management strategy for hybrid power ships with hybrid energy storage system. J Energy Storage Aug. 2022;52. https://doi.org/10.1016/j.est.2022.104763.
[27] Powade R, Bhateshvar Y. Design of semi-actively controlled battery-supercapacitor hybrid energy storage system. Mater Today Proc Jan. 2023;72:1503–9. https://doi.org/10.1016/j.matpr.2022.09.378.
[28] Li H, et al. Collaborative optimization of VRB-PS hybrid energy storage system for large-scale wind power grid integration. Energy 2023;265(Feb). https://doi.org/10.1016/j.energy.2022.126292.
[29] Marocco P, Ferrero D, Lanzini A, Santarelli M. The role of hydrogen in the optimal design of off-grid hybrid renewable energy systems. J Energy Storage 2022;46:103893. https://doi.org/10.1016/j.est.2021.103893.
[30] Jin C, Xiao J, Hou J, Wu X, Zhang J, Du E. Flexibility improvement evaluation of hydrogen storage based on electricity–hydrogen coupled energy model. Global Energy Interconnection Aug. 2021;4(4):371–83. https://doi.org/10.1016/j.gloei.2021.09.004.

Please cite this article as: Martinez Alonso A et al., Multi-state optimal power dispatch model for power-to-power systems in off-grid hybrid energy systems: A case study in Spain, International Journal of Hydrogen Energy, https://doi.org/10.1016/j.ijhydene.2023.06.019

[31] Rabiee A, Keane A, Soroudi A. Green hydrogen: a new flexibility source for security constrained scheduling of power systems with renewable energies. Int J Hydrogen Energy May 2021;46(37):19270–84. https://doi.org/10.1016/j.ijhydene.2021.03.080.
[32] Gracia L, Casero P, Bourasseau C, Chabert A. Use of hydrogen in off-grid locations, a techno-economic assessment. Energies (Basel) Nov. 2018;11(11). https://doi.org/10.3390/en11113141.
[33] Cozzolino R, Tribioli L, Bella G. Power management of a hybrid renewable system for artificial islands: a case study. Energy 2016;106:774–89. https://doi.org/10.1016/j.energy.2015.12.118.
[34] Okundamiya MS. Size optimization of a hybrid photovoltaic/fuel cell grid connected power system including hydrogen storage. Int J Hydrogen Energy Aug. 2021;46(59):30539–46. https://doi.org/10.1016/j.ijhydene.2020.11.185.
[35] Schöne N, Khairallah J, Heinz B. Model-based techno-economic evaluation of power-to-hydrogen-to-power for the electrification of isolated African off-grid communities. Energy for Sustainable Development Oct. 2022;70:592–608. https://doi.org/10.1016/j.esd.2022.08.020.
[36] Mancarella P. MES (multi-energy systems): an overview of concepts and evaluation models. Energy Feb. 2014;65:1–17. https://doi.org/10.1016/J.ENERGY.2013.10.041.
[37] Lu Z, Li Y, Zhuo G, Xu C. Configuration optimization of hydrogen-based multi-microgrid systems under electricity market trading and different hydrogen production strategies. Sustainability Apr. 2023;15(8):6753. https://doi.org/10.3390/su15086753.
[38] Luna AC, Diaz NL, Graells M, Vasquez JC, Guerrero JM. Mixed-integer-linear-programming-based energy management system for hybrid PV-wind-battery microgrids: modeling, design, and experimental verification. IEEE Trans Power Electron 2017;32(4):2769–83. https://doi.org/10.1109/TPEL.2016.2581021.
[39] Valverde L, Bordons C, Rosa F. Integration of fuel cell technologies in renewable-energy-based microgrids optimizing operational costs and durability. IEEE Trans Ind Electron 2016;63(1):167–77. https://doi.org/10.1109/TIE.2015.2465355.
[40] Javadi MS, Esmaeel Nezhad A, Sabramooz S. Economic heat and power dispatch in modern power system harmony search algorithm versus analytical solution. Sci Iran 2012;19(6):1820–8. https://doi.org/10.1016/j.scient.2012.10.033.
[41] Felice A, Rakocevic L, Peters L, Messagie M, Coosemans T, Camargo LR. Renewable energy communities: do they have a business case in Flanders?. 2022 [Online]. Available: http://arxiv.org/abs/2202.05151.
[42] Javadi MS, et al. A two-stage joint operation and planning model for sizing and siting of electrical energy storage devices considering demand response programs. Int J Electr Power Energy Syst Jun. 2022;138. https://doi.org/10.1016/j.ijepes.2021.107912.
[43] Hassan Q, Abdulrahman IS, Salman HM, Olapade OT, Jaszczur M. Techno-economic assessment of green hydrogen production by an off-grid photovoltaic energy system. Energies (Basel) Jan. 2023;16(2). https://doi.org/10.3390/en16020744.
[44] Ju L, et al. Robust Multi-objective optimal dispatching model for a novel island micro energy grid incorporating biomass waste energy conversion system, desalination and power-to-hydrogen devices. Appl Energy Aug. 2023;343. https://doi.org/10.1016/j.apenergy.2023.121176.
[45] Zhang H, Wang J, Zhao X, Yang J, Bu sinnah ZA. Modeling a hydrogen-based sustainable multi-carrier energy system using a multi-objective optimization considering embedded joint chance constraints. Energy Sep. 2023;278. https://doi.org/10.1016/j.energy.2023.127643.
[46] Kilic M, Altun AF. Dynamic modelling and multi-objective optimization of off-grid hybrid energy systems by using battery or hydrogen storage for different climates. Int J Hydrogen Energy 2023. https://doi.org/10.1016/j.ijhydene.2022.12.103.
[47] Ao Y, Laghrouche S, Depernet D, Chen K. Lifetime prediction for proton exchange membrane fuel cell under real driving cycles based on platinum particle dissolve model. Int J Hydrogen Energy 2020;45(56):32388–401. https://doi.org/10.1016/j.ijhydene.2020.08.188.
[48] Weiß A, Siebel A, Bernt M, Shen T-H, Tileli V, Gasteiger HA. Impact of intermittent operation on lifetime and performance of a PEM water electrolyzer. J Electrochem Soc 2019;166(8):F487–97. https://doi.org/10.1149/2.0421908jes.
[49] Baumhof MT, Raheli E, Johnsen AG, Kazempour J. Optimization of hybrid power plants: when is a detailed electrolyzer model necessary?. Jan. 2023 [Online]. Available: http://arxiv.org/abs/2301.05310.
[50] Evins R, Orehounig K, Dorer V, Carmeliet J. New formulations of the 'energy hub' model to address operational constraints. Energy Aug. 2014;73:387–98. https://doi.org/10.1016/j.energy.2014.06.029.
[51] Matute G, Yusta JM, Correas LC. Techno-economic modelling of water electrolysers in the range of several MW to provide grid services while generating hydrogen for different applications: a case study in Spain applied to mobility with FCEVs. Int J Hydrogen Energy 2019;44(33):17431–42. https://doi.org/10.1016/j.ijhydene.2019.05.092.
[52] Matute G, Yusta JM, Beyza J, Correas LC. Multi-state techno-economic model for optimal dispatch of grid connected hydrogen electrolysis systems operating under dynamic conditions. Int J Hydrogen Energy 2021;46(2):1449–60. https://doi.org/10.1016/j.ijhydene.2020.10.019.
[53] Wei F, Sui Q, Li X, Lin X, Li Z. Optimal dispatching of power grid integrating wind-hydrogen systems. Int J Electr Power Energy Syst Feb. 2021;125. https://doi.org/10.1016/j.ijepes.2020.106489.
[54] Pardhi S, Chakraborty S, Tran DD, El Baghdadi M, Wilkins S, Hegazy O. A review of fuel cell powertrains for long-haul heavy-duty vehicles: technology, hydrogen, energy and thermal management solutions. Energies Dec. 01, 2022;15(24). https://doi.org/10.3390/en15249557. MDPI.
[55] Dispatching fuel-cell hybrid electric vehicles toward transportation and energy systems integration. CSEE Journal of Power and Energy Systems 2021. https://doi.org/10.17775/cseejpes.2020.03640.
[56] Abdelghany MB, Shehzad MF, Liuzza D, Mariani V, Glielmo L. Optimal operations for hydrogen-based energy storage systems in wind farms via model predictive control. Int J Hydrogen Energy 2021;46(57):29297–313. https://doi.org/10.1016/j.ijhydene.2021.01.064.
[57] Viteri JP, Viteri S, Alvarez-Vasco C, Henao F. A systematic review on green hydrogen for off-grid communities –technologies, advantages, and limitations. Int J Hydrogen Energy 2023. https://doi.org/10.1016/j.ijhydene.2023.02.078. Elsevier Ltd.
[58] Gobierno de Canarias. Anuario del sector eléctrico de Canarias 2019. 2020. p. 340.
[59] Red Electrica de España. Informe del Sistema Eléctrico Español 2020. 2020.
[60] Copernicus. European Union's Earth observation programme. 2021 [Online]. Available: https://www.copernicus.eu/en/about-copernicus.

Please cite this article as: Martinez Alonso A et al., Multi-state optimal power dispatch model for power-to-power systems in off-grid hybrid energy systems: A case study in Spain, International Journal of Hydrogen Energy, https://doi.org/10.1016/j.ijhydene.2023.06.019

[61] Larsson P, Borjesson P. Cost models for battery energy storage systems. kTH Industrial Engineering and Management; 2018. p. 31 [Online]. Available: http://www.diva-portal.org/smash/get/diva2:1254196/FULLTEXT01.pdf.
[62] Kebede AA, et al. Techno-economic analysis of lithium-ion and lead-acid batteries in stationary energy storage application. J Energy Storage 2021;40:102748. https://doi.org/10.1016/j.est.2021.102748.
[63] Jiang T. Development of alkaline electrolyzer electrodes and their characterization in overall water splitting. 2021.
[64] Hyjack : Hydrogen. Online, https://hyjack.tech/. [Accessed 29 April 2022].
[65] Chadly A, Azar E, Maalouf M, Mayyas A. Techno-economic analysis of energy storage systems using reversible fuel cells and rechargeable batteries in green buildings. Energy 2022;247:123466. https://doi.org/10.1016/j.energy.2022.123466.
[66] Cummins. Catalogue and specification sheet Diesel generator set QSB5 series engine 50-125 kW @ 60Hz EPA Tier 3 emissions. 2016.

Please cite this article as: Martinez Alonso A et al., Multi-state optimal power dispatch model for power-to-power systems in off-grid hybrid energy systems: A case study in Spain, International Journal of Hydrogen Energy, https://doi.org/10.1016/j.ijhydene.2023.06.019